Title

Anatomic and dosimetric changes in patients with head and neck cancer treated with an integrated MRI-tri-60Co teletherapy device

Journal

British Journal of Radiology, 89(1067)

ISSN

0007-1285

Authors

Raghavan, Govind
Kishan, Amar U
Cao, Minsong
et al.

Publication Date

2016-11-01

DOI

10.1259/bjr.20160624

Peer reviewed

BJR

Received: 18 July 2016 | Revised: 25 August 2016 | Accepted: 20 September 2016

http://dx.doi.org/10.1259/bjr.20160624

Cite this article as:
Raghavan G, Kishan AU, Cao M, Chen AM. Anatomic and dosimetric changes in patients with head and neck cancer treated with an integrated MRI-tri-^{60}Co teletherapy device. *Br J Radiol* 2016; **89**: 20160624.

FULL PAPER

Anatomic and dosimetric changes in patients with head and neck cancer treated with an integrated MRI-tri-^{60}Co teletherapy device

GOVIND RAGHAVAN, BS, AMAR U KISHAN, MD, MINSONG CAO, PhD and ALLEN M CHEN, MD

Department of Radiation Oncology, University of California, Los Angeles, David Geffen School of Medicine, Los Angeles, CA, USA

Address correspondence to: Dr Allen M Chen
E-mail: *achen5@kumc.edu*

Objective: Prior studies have relied on CT to assess alterations in anatomy among patients undergoing radiation for head and neck cancer. We sought to determine the feasibility of using MRI-based image-guided radiotherapy to quantify these changes and to ascertain their potential dosimetric implications.

Methods: 6 patients with head and neck cancer were treated with intensity-modulated radiotherapy (IMRT) on a novel tri-^{60}Co teletherapy system equipped with a 0.35-T MRI (VR, ViewRay Incorporated, Oakwood Village, OH) to 66–70 Gy in 33 fractions (fx). Pre-treatment MRIs on Fx 1, 5, 10, 15, 20, 25, 30 and 33 were imported into a contouring interface, where the primary gross tumour volume (GTV) and parotid glands were delineated. The centre of mass (COM) shifts for these structures were assessed relative to Day 1. Dosimetric data were co-registered with the MRIs, and doses to the GTV and parotid glands were assessed.

Results: Primary GTVs decreased significantly over the course of IMRT (median % volume loss, 38.7%; range, 29.5–72.0%; $p < 0.05$) at a median rate of 1.2%/fx (range, 0.92–2.2%/fx). Both the ipsilateral and contralateral parotid glands experienced significant volume loss ($p < 0.05$, for all) and shifted medially during IMRT. Weight loss correlated significantly with parotid gland volume loss and medial COM shift ($p < 0.05$).

Conclusion: Integrated on-board MRI can be used to accurately contour and analyze primary GTVs and parotid glands over the course of IMRT. COM shifts and significant volume reductions were observed, confirming the results of prior CT-based exercises.

Advances in knowledge: The superior resolution of on-board MRI may facilitate online adaptive replanning in the future.

INTRODUCTION

Radiation therapy plays a critical role in the management of head and neck cancers with recent technological advances improving its efficiency and safety. Intensity-modulated radiotherapy (IMRT) allows high doses to be conformed to target lesions, leaving adjacent normal tissues relatively spared.[1–3] Improvements in image-guided radiation therapy (IGRT) have simultaneously allowed reduction in planning margins, further reducing dose to normal tissue and increasing confidence in the accuracy of IMRT treatments.[2,3]

Several studies have documented anatomical changes during the course of IMRT in patients with head and neck cancer, quantifying regression and spatial shifts of tumours and organ at risk (OAR).[4–10] Interfractional anatomical changes, in turn, can substantially alter dose deposition, suggesting a benefit to adaptive replanning.[7–19] However, adaptive replanning remains to be widely adopted owing to its time-intensive nature and an unclear threshold of anatomical changes required for its posited benefit.[10,11,16,20] The aforementioned studies of anatomical alteration during IMRT relied on CT imaging, which might not provide optimal soft-tissue contrast/resolution, leading to possible interobserver variability.[21,22] MRI provides superior soft-tissue resolution,[2,21,23,24] potentially allowing for a more accurate evaluation of anatomical changes during IMRT.

Using a recently developed, commercially available tri-^{60}Co teletherapy platform (VR, ViewRay Incorporated, Oakwood Village, OH), it is possible to obtain daily MR images with an on-board 0.35-T MRI.[25] The purpose of this study was to use serial MR images to quantify anatomical changes in gross tumour volume (GTV) and parotid glands over the course of IMRT in patients with head and neck squamous cell carcinoma (HNSCC) and assess the dosimetric consequences of these changes.

METHODS AND MATERIALS

Patients, treatment planning and delivery

Six consecutive patients with HNSCC who were treated with ViewRay (VR) from February to July 2015 were retrospectively identified. Clinical information, including weight, was extracted from the electronic medical record. This study was performed with institutional review board approval (Institutional review board 14–000340).

Each patient received IMRT *via* VR in 33 fractions (fx) with total dosage to the primary GTV ranging from 66 to 70 Gy. Patients were immobilized with a custom Type-S Head, Neck & Shoulder thermoplastics AquaPlast masks to minimize setup variation. Simulation scans were obtained on the VR without contrast. Patient characteristics are shown in Table 1.

Imaging

Daily setup MRIs were acquired at 1.5-mm isotropic spatial resolution and 172-s acquisition time using a balanced steady-state coherent sequence (True fast imaging with steady state precision (TrueFISP) sequence) before each treatment delivery. This imaging was part of the normal patient setup protocol. No online adaptive replanning was performed. Pre-treatment MRIs on Days 1, 5, 10, 15, 20, 25, 30 and 33, along with planning imaging, were obtained.

Contouring

All image sets were imported into MIM software (MIMvista Corporation, Cleveland, OH) for contouring. Each fx imaging was fused with the planning MRI. The primary GTV and the ipsilateral and contralateral parotids were manually contoured on each axial slice for every fx. For the purpose of this study, the GTV was defined as the primary tumour only; grossly visible lymph nodes were not included. All contouring was performed by a single individual (GR) and verified by a board-certified radiation oncologist specializing in head and neck malignancies (AMC). Primary GTV and parotid gland volumes were quantified using MIM.

Centre of mass assessment

To determine the centre of mass (COM) shifts of the primary GTVs as well as the ipsilateral and contralateral parotid glands during treatment, daily imaging was fused with imaging from Day 1 in MIM. The COM on Day 1 was used as the reference point and displacements relative to this fixed reference on subsequent fx were assessed in the mediolateral direction. The COM from Fx 1, rather than the planning MRI, was chosen as the reference point to reduce the impact of any potential changes that occurred between simulation and treatment initiation (<7 days). The COM was defined automatically by the MIM software as the coordinates corresponding to the volumetric centre of the contour in question.

Statistical analysis

Percent decrease in volume was calculated as: $[(\text{Volume}_{\text{Day1}} - \text{Volume}_{\text{Day33}})/(\text{Volume}_{\text{Day1}})] \times 100$. Rate of volume loss as a percentage of initial volume was determined as follows: $[(\text{Volume}_{\text{Day1}} - \text{Volume}_{\text{Day33}})/(32 \quad \text{fx})/(\text{Volume}_{\text{Day1}})] \times 100$. Because pre-treatment MRI was obtained on Day 33, the analysis involved only 32 fx. The paired, two-tailed *t*-test was used to assess differences over a course of IMRT, and Spearman's correlation coefficient (R) was used to assess the strength of all correlations.

Daily dosimetric data were imported from VR into MIM and overlaid onto daily pre-treatment MRIs. For each fraction, the mean dose and % of the ipsilateral and contralateral parotid gland receiving >0.91 (30 Gy/33 fx) was then assessed. The % of primary GTV receiving the prescribed dose each fx, dose/33 fx ($V_{100\%}$) for the primary GTVs was determined.

RESULTS

Primary gross tumour volume changes

GTV changes over the course of IMRT are shown in Figure 1a. GTV decreased significantly (median, 38.7%; range, 29.5–72.0%; $p < 0.05$). Smaller tumours experienced less absolute reduction than larger tumours. Median rate of volume loss as a percentage of initial volume was 1.2%/fx (range, 0.99–2.2%/fx). For non-recurrent tumours, median percentage volume loss was 52.7% (29.5–72.0%) and reduction rate was 1.6%/fx (0.92–2.2%/fx). For recurrent tumours, median percentage volume reduction was 32.0% (31.6–45.4%) and rate of loss was

Table 1. Patient clinical characteristics

Patient number	Age	Gender	Stage	Site	p16 status	Dose (Gy)/fx	Concurrent chemotherapy
1	66	M	T3N1M0/III	Right BOT	Positive	69.96/33	Yes
2	47	M	T4aN1M0/IVA	Left BOT	Positive	69.96/33	Yes
3	73	M	T4aN2bM0/IVA	Left BOT	N/A	69.96/33	Yes
4	51	F	Recurrent/ T4N1M0/IVA	Left nasopharynx	N/A	66.00/33	No
5	44	M	Recurrent/ T4N0M0/IVA	Left maxillary sinus	N/A	66.00/33	No
6	73	M	Recurrent/ T2N2bM0/IVA	Right oropharynx	Negative	66.00/33	No

BOT, base of tongue; F, female; fx, fraction; M, male; N/A, not available.
Patients on chemotherapy were given weekly cisplatin. P16 status was a marker for human papilloma virus status.

Figure 1. (a) Primary gross tumour volumes (GTVs) on each treatment day are presented as a percentage of the initial volume on Day 1. Volume loss was significant ($p < 0.05$). (b) Centre of mass (COM) shift was reported as the magnitude of shift in the mediolateral axis. Numbers in the figure legend correspond to patient numbers in Table 1.

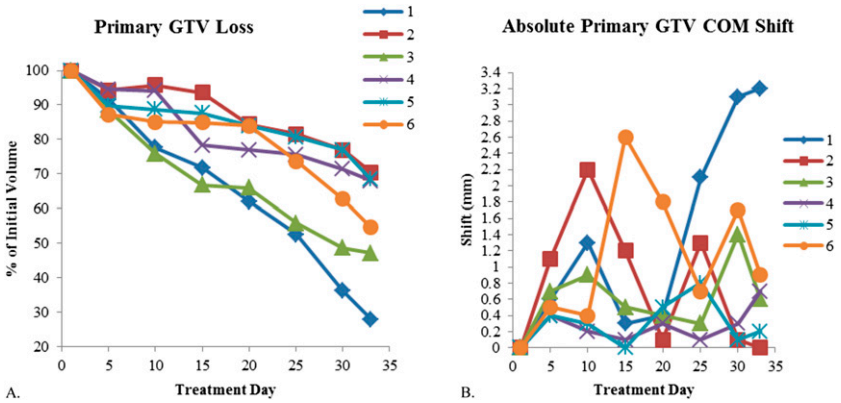

1.0%/fx (0.99–1.4%/fx). Median absolute COM shift on Day 33 relative to Day 1 was 0.65 mm (0–3.2 mm) (Figure 1b).

Parotid gland volume changes

Patient 6 had a prior parotidectomy, leaving only the contralateral parotid gland. Significant volume reduction of ipsilateral parotids occurred ($p < 0.05$) (Figure 2a). Median % volume loss was 31.1% (2.3–43.9%) and median rate of volume loss was 0.97%/fx (0.07–1.4%/fx). Including only the base of tongue tumours (Patients 1–3), median ipsilateral percentage volume loss was 39.2% (31.1–43.9%) with a median relative reduction rate of 1.2%/fx (0.97–1.4%/fx). The remaining two patients experienced percentage volume reductions of 2.3% (rate: 0.07%/fx) and 4.5% (rate: 0.14%/fx), respectively.

Contralateral parotid glands also shrank significantly between the first and final fx ($p < 0.05$) (Figure 2b), with a median percentage volume loss of 21.8% (4.0–40.5%) and median shrinkage rate of 0.68%/fx (0.12–1.3%/fx). Contralateral parotids in Patients 1–3 and 6 had a median relative volume loss of 29.0% (20.3–40.5%) and a median relative rate loss of 0.91%/fx (0.63–1.3%/fx). Patients 4 and 5 underwent contralateral parotid volume shrinkage of 7.1% (rate: 0.22%/fx) and 4.0% (rate: 0.13%/fx), respectively. There was no significant difference in volume loss between ipsilateral and contralateral parotid glands during IMRT ($p > 0.05$).

Parotid gland centre of mass shifts

Both parotid glands generally shifted medially over the course of treatment (Figure 2c,d). By Day 33, there was a median medial shift of 0.9 mm (−1.9–4.5 mm) for the ipsilateral and 1.4 mm (−0.4–4 mm) for the contralateral parotid glands. Patient 5's ipsilateral parotid gland appeared to shift laterally, while the contralateral parotids in Patients 4 and 5 shifted slightly laterally by the end of IMRT. No significant difference was found between ipsilateral and contralateral parotid shifts ($p > 0.05$).

Weight loss correlation

Correlation between patient weight loss and anatomical changes was determined by Spearman's correlation coefficient (Figure 3). Weight loss correlated with percentage volume loss of both parotids combined ($R = 0.72$, $p < 0.05$). Separately, weight loss correlated with ipsilateral ($R = 0.9$, $p < 0.05$) but not contralateral ($R = 0.49$, $p > 0.05$) parotid gland volume reduction. Medial shift of both parotids together correlated with weight loss ($R = 0.68$, $p < 0.05$) while separately, neither ipsilateral nor contralateral shift aligned with weight loss. Weight loss did not correlate with GTV COM shift ($R = 0.43$, $p > 0.05$) or volume loss ($R = 0.09$, $p > 0.05$).

Dosimetry

Doses to the parotids and GTVs were determined for each fx (Figure 4). Median difference between planning dose per fx and administered mean dose at Fx 33 was 0.008 Gy (−0.06–0.18 Gy) for ipsilateral and 0.01 Gy (−0.12–0.27 Gy) for contralateral parotid glands. For the % of parotid gland receiving >0.91 Gy (30 Gy/33 fx) each fx, median difference between planned dose per fx and administered dose at Fx 33 was 0% (−3.28–11.18%) for ipsilateral and −0.07% (−9.6–26.7%) for contralateral parotid glands. Regarding the primary GTVs, there was a median difference in $V_{100\%}$ between planned and administered dose at Fx 33 of 0.2% (−0.37–2.6%). No statistical significance was found for these data. Planning dose to the parotid glands correlated with percentage volume loss ($R = 0.76$, $p < 0.01$) (Figure 5).

DISCUSSION

This study used daily imaging from a novel tri-^{60}Co teletherapy platform with integrated MRI to quantify the anatomic variation occurring over the course of IMRT in patients with HNSCC. Consistent with prior CT-based observational studies, we found that the primary GTVs decreased in volume significantly by the end of IMRT, with a median volume reduction of 38.7% and a median rate of reduction of 1.2%/fx. The wide ranges indicate that tumour response is not uniform and subject to unpredictable patterns of regression.[4,8,10,22] Using daily CT scans, Barker et al observed a median rate of loss for primary tumours of 1.7% per day,[4] and Chen et al[22] found a mean % volume reduction for human papilloma virus positive oropharyngeal GTVs of 57.5%. Although limited by sample size, our study

Figure 2. (a) Ipsilateral and (b) contralateral parotid gland volume loss as measured on treatment Fractions 1, 5, 10, 15, 20, 25, 30 and 33, and volumes are plotted as a percentage of volume on Day 1. (c) Ipsilateral and (d) contralateral parotid gland centre of mass (COM) shifts as measured in the mediolateral direction on treatment days relative to the COM on Day 1. A medial shift was considered positive and a lateral shift negative when plotted. Numbers in the figure legend correspond to patient numbers in Table 1.

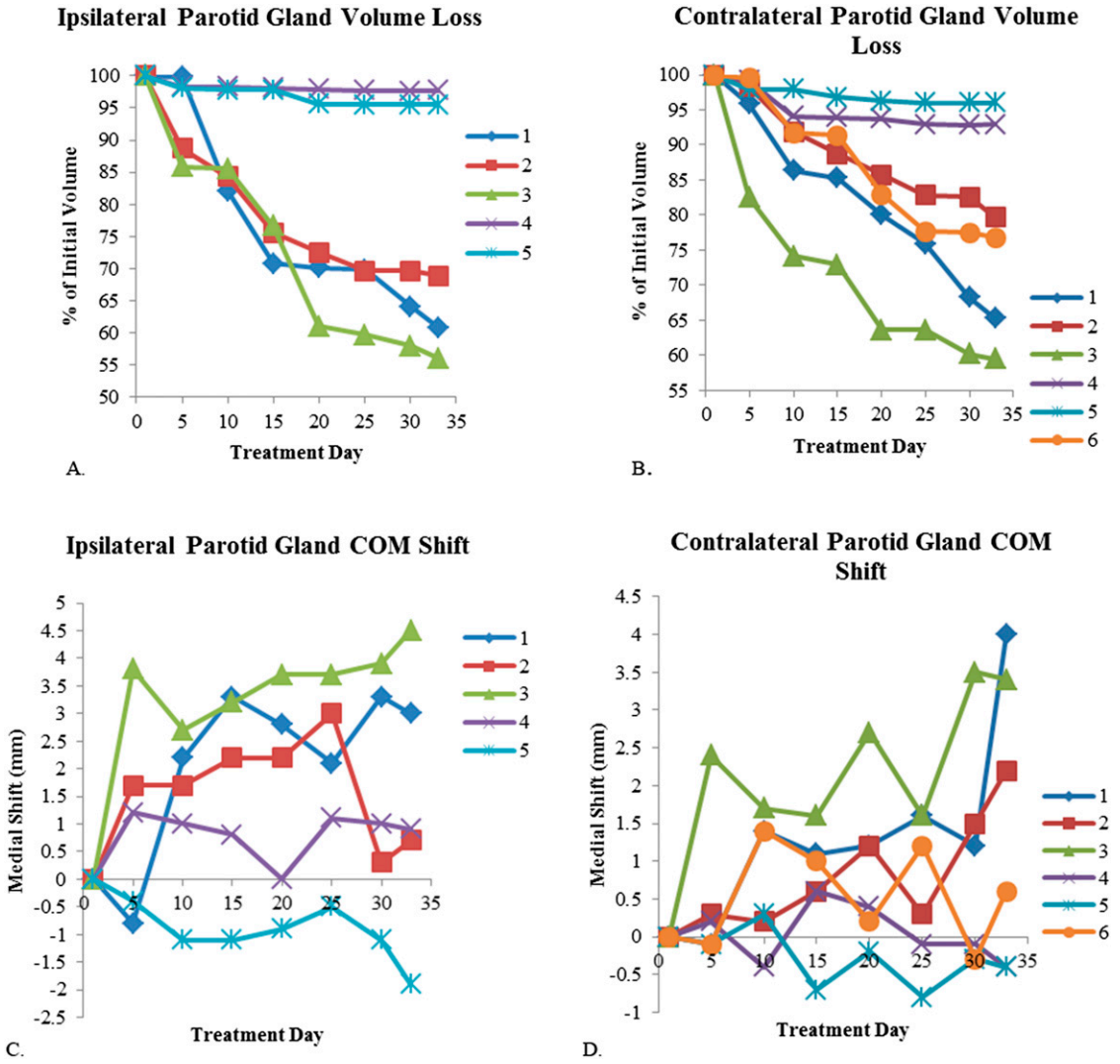

included two patients who were human papilloma virus positive with base of tongue tumours and mean percentage reduction of 50.1%, indicating similar findings. In one of the only studies using MRI, Kamran et al[26] similarly found that primary tumour volumes declined by a median amount of 33% at 6 weeks (17–75%). We also observed that GTV COMs shifted in a non-uniform pattern between fx likely dependent on tumour location. Others also previously found GTV COMs to shift throughout IMRT.[4,10] Differences in findings may be due to imaging modalities, tumour characteristics, variability in weight loss and heterogeneous treatment plans.

In addition, the parotid glands diminished considerably in volume by the completion of IMRT. Ipsilateral parotid glands decreased by a median amount of 31.1% at a median rate of 0.97%/fx, while contralateral parotids declined by 21.8% at a rate of 0.68%/fx. In the majority of patients, it appeared that the ipsilateral parotid gland shrank to a larger extent and at a faster rate than the contralateral parotid gland, which was expected owing to higher planned dose. Both planning dose and weight loss correlated with parotid shrinkage, indicating that the two factors combined to contribute to parotid gland volume loss. Lower planning dose, location further away from the primary GTV and minimal weight change accounted for the two patients (4 and 5) who did not experience similar magnitudes of parotid gland shrinkage as the others. Our results are in remarkable agreement with prior studies, which reported median parotid shrinkage rates of 0.6% per day (0.2–1.8% per day)[4] and 0.7% per day (0.4–1.3% per day),[5] found a mean volume reduction of 30.2% (17.1–55.8%) for ipsilateral and 17.5% (15.6–48.5%) for contralateral parotid glands[9] and correlated parotid gland shrinkage with both weight loss[27] and planned dose.[6]

Figure 3. Weight loss between Fractions 1 and 33 of intensity-modulated radiotherapy correlated with both parotid gland volume loss (a) and parotid gland medial centre of mass shift (b) by Spearman's correlation [for (a), $R = 0.72$ and $p < 0.05$; for (b), $R = 0.68$ and $p < 0.05$]. Both ipsilateral and contralateral parotids were included in the correlation calculations and plots.

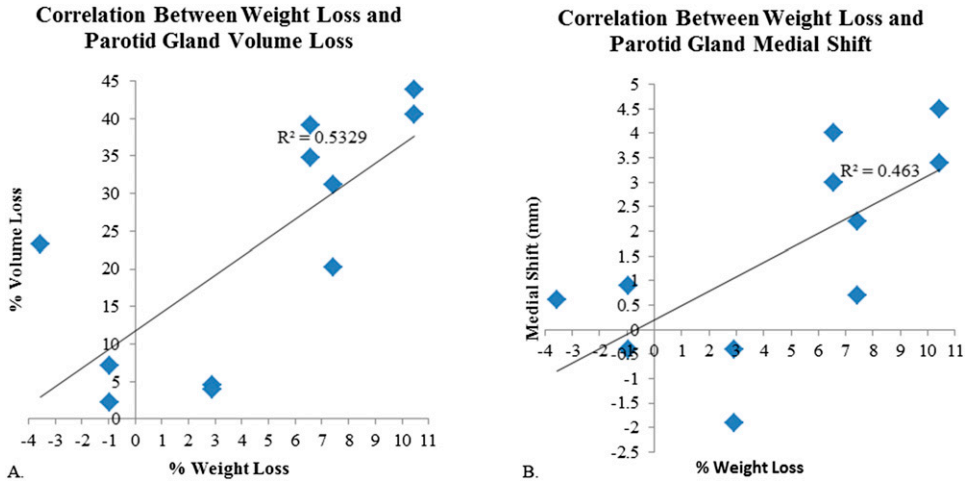

Both ipsilateral and contralateral parotid glands generally shifted medially by the end of treatment. This finding is consistent with the literature, as multiple studies have identified that the parotid glands displace medially, likely owing to alterations in muscle and fat distribution combined with changes in body mass index.[4–7,10] Barker et al[4] reported a median medial shift of

Figure 4. Dosimetric analysis was conducted in regard to the dosage received by the parotid glands and gross tumour volumes (GTVs) over the course of intensity-modulated radiotherapy (IMRT): in (a) and (b), the mean dose administered to the ipsilateral and contralateral parotid glands in each fraction (fx) is shown. Mean dose at treatment Fx 0 is the planned dose per fx. In (c), the % of primary GTV receiving the prescribed dose each fx, dose/33 fx, ($V_{100\%}$) for the primary GTVs during IMRT is displayed. Dose did not change significantly over radiotherapy (RT). Numbers in the figure legends correspond to patient numbers in Table 1.

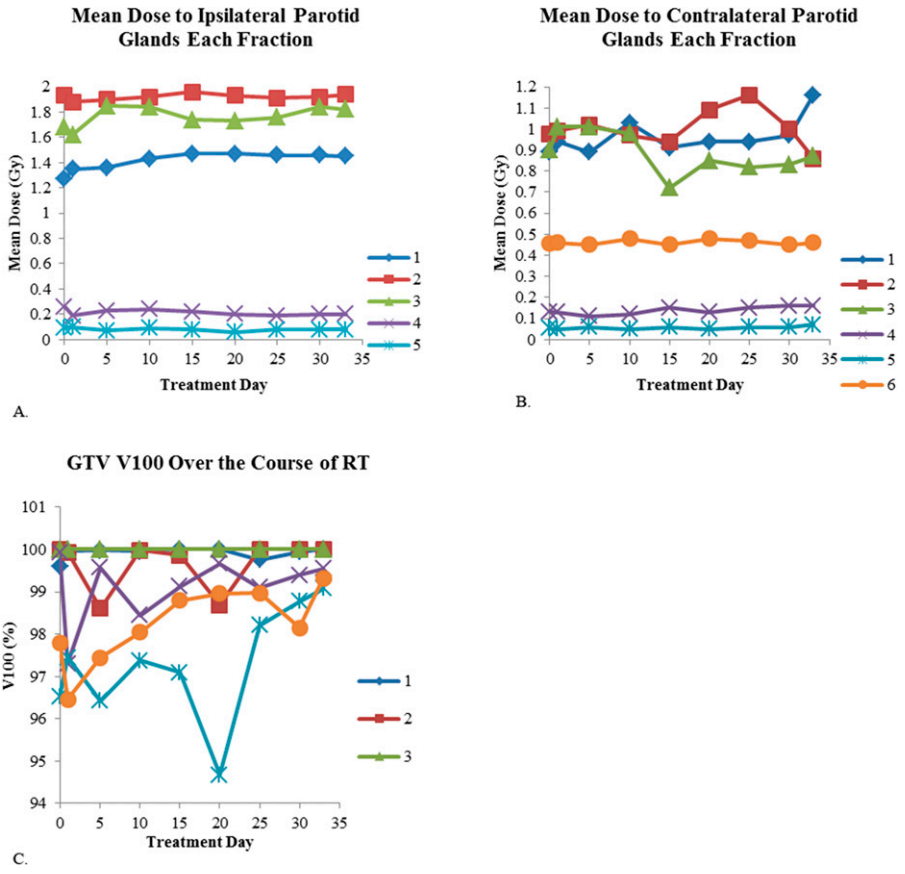

Figure 5. Planned dose to the parotid glands correlated with parotid volume loss by Spearman's correlation ($R = 0.76$ and $p < 0.01$). Both ipsilateral and contralateral parotids were included in the calculation and plot.

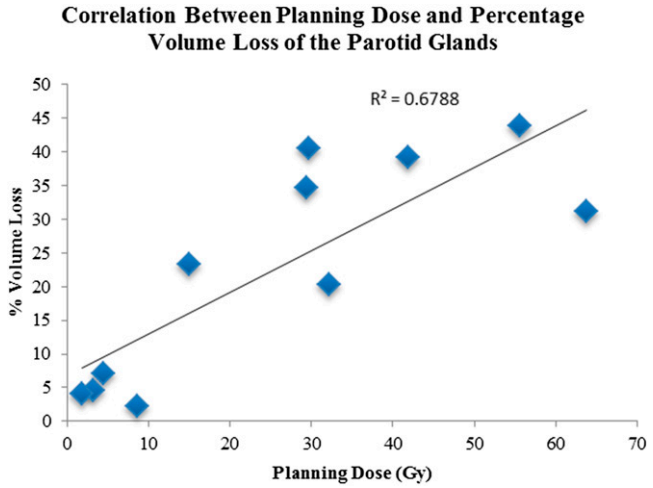

3.1 mm (−0.3–9.9 mm), and Castadot et al[10] determined ipsilateral parotids to shift medially by a mean of 3.4 mm. Although we saw similar trends, the overall medial shift was not as high owing to the heterogeneous patient population. In addition, the apparent lateral shift of the parotid glands in Patients 4 and 5 may be due to salivary stasis or inflammation. Overall, the medial shift of the parotid glands correlated with weight loss, confirming the findings of Barker et al.[4]

Other studies have attempted to correlate anatomic changes with dosimetric analysis and discussed the potential benefits of replanning in head and neck cancers.[7–13,15,17,19] As the parotid glands shift medially during IMRT, they may be exposed to higher than expected levels of radiation and consequently an increased probability of xerostomia.[8,10–12,14] Although several studies have found that adaptive replanning may potentially reduce dosage to the parotids, the appropriate means of selection remain elusive.[11,13,15,17,19] While our results did not identify any significant changes in parotid dose over the course of IMRT, this conclusion is limited by the heterogeneous patient population and the lack of cumulative dosage data.

Regardless, there are several explanations for this finding. Others have found that the medial aspects of the parotid glands stay relatively fixed while the lateral parts shift medially.[6,28] In this scenario, if the medial lobe of the parotid gland were already in a low-dose region, the overall change in parotid dosimetry would be negligible. Furthermore, tight planning margins were used such that even if the parotid glands shifted medially, they may not have entered a high-dose region. Finally, it is possible that the precise IGRT afforded by the VR's daily MRI capabilities allowed for improved registration to the primary tumour, thereby limiting unanticipated doses to OARs. Enhanced IGRT could also explain why $V_{100\%}$ to the GTV was maintained.

Although some studies show adaptive replanning to be clinically beneficial,[16,18,20] the technique has not been widely adopted largely owing to its resource and time-intensive nature. In addition, a consensus does not exist as to who would clinically benefit from replanning.[10,11,16,19,20] Based on the dosimetric results of our study, it is unlikely that uniformly recommending adaptive replanning would have resulted in clinical benefit with regard to the parotids and primary GTVs. However, our population was quite heterogeneous, and it is uncertain whether the same conclusion regarding the dosimetric impact would have been reached without the added benefit of MRI-guided IGRT and tight planning margins.

The topic of geometric distortion is an important issue to be addressed when using MRI for contouring and treatment planning. As presented in the recent review article by Weygand et al,[29] the geometric distortion is a function of the magnetic field strength and gradient strength, *i.e.* higher magnetic field suffers larger geometric distortion and increased gradient strength results in reduced geometric distortion. As shown by Stanescu et al,[30] the maximum distortion at nasal sinus air cavities is about 0.6 mm for a 0.5-T magnetic field with a gradient strength of 5 $mT\,m^{-1}$.[30] The VR MRI system has a smaller magnetic field (0.35 T) with a much higher gradient strength (18 $mT\,m^{-1}$).[25] It is reasonable to believe that the magnetic susceptibility-induced geometric distortion for the MRI system used in the study is not a major concern for contouring. Nonetheless, it is possible that the overall system and patient-related geometric distortion introduced uncertainty, as mean distortions of 2.2 mm have been documented at field strengths as low as 0.2 T.[31] Algorithms to mitigate this effect have been developed and evaluation of this will be the subject of future study.[32] Phantom measurements were also performed on our system, and the results indicated geometric accuracy of 1 mm within the 20-cm imaging field of view for head and neck imaging.

This study had several limitations. First, the sample size was small. However, all patients with HNSCC treated with the VR in this consecutive series were included. Second, some studies have suggested that the submandibular glands, rather than the parotid glands, are the relevant OARs for xerostomia.[33] As most prior studies on anatomic changes during radiotherapy have focused on the GTV and parotid, we similarly focused on these targets for the purposes of comparative analysis. In future work, we will examine dosimetric changes to the submandibular gland as well. In addition, the tumours were heterogeneous, which may affect radiation response. Tumour volumes were contoured based on visual appearance on MRIs. However, no functional imaging was performed, which could lead to a better understanding of tumour regression and improved volume determination. Finally, although MRI provides superior soft-tissue resolution, manual contouring does not allow for 100% accuracy. Even with 1.5–3-T strength MRIs, it can be challenging to discern the margin of infiltrative tumours, particularly in the presence of treatment-induced inflammation. The uncertainties introduced by this issue are likely tempered somewhat by the fact that all contours were approved by a single radiation oncologist specializing in head and neck malignancies.

CONCLUSION

This study was among the first to use daily MRIs to quantify the ongoing interfraction anatomic changes among patients receiving IMRT for head and neck cancer and demonstrates the feasibility of this technology for future work. The data indicate that anatomic changes take place, particularly with respect to the primary tumour volume and parotid glands, during IMRT but significant dosimetric shifts were not always apparent.

REFERENCES

1. Lee N, Puri DR, Blanco AI, Chao KS. Intensity-modulated radiation therapy in head and neck cancers: an update. *Head Neck* 2007; **29**: 387–400. doi: http://dx.doi.org/10.1002/hed.20332
2. Xing L, Thorndyke B, Schreibmann E, Yang Y, Li TF, Kim GY, et al. Overview of image-guided radiation therapy. *Med Dosim* 2006; **31**: 91–112. doi: http://dx.doi.org/10.1016/j.meddos.2005.12.004
3. Baskar R, Lee KA, Yeo R, Yeoh KW. Cancer and radiation therapy: current advances and future directions. *Int J Med Sci* 2012; **9**: 193–9. doi: http://dx.doi.org/10.7150/ijms.3635
4. Barker JL Jr, Garden AS, Ang KK, O'Daniel JC, Wang H, Court LE, et al. Quantification of volumetric and geometric changes occurring during fractionated radiotherapy for head-and-neck cancer using an integrated CT/linear accelerator system. *Int J Radiat Oncol Biol Phys* 2004; **59**: 960–70. doi: http://dx.doi.org/10.1016/j.ijrobp.2003.12.024
5. Lee C, Langen KM, Lu W, Haimerl J, Schnarr E, Ruchala KJ, et al. Evaluation of geometric changes of parotid glands during head and neck cancer radiotherapy using daily MVCT and automatic deformable registration. *Radiother Oncol* 2008; **89**: 81–8. doi: http://dx.doi.org/10.1016/j.radonc.2008.07.006
6. Vasquez Osorio EM, Hoogeman MS, Al-Mamgani A, Teguh DN, Levendag PC, Heijmen BJ. Local anatomic changes in parotid and submandibular glands during radiotherapy for oropharynx cancer and correlation with dose, studied in detail with nonrigid registration. *Int J Radiat Oncol Biol Phys* 2008; **70**: 875–82. doi: http://dx.doi.org/10.1016/j.ijrobp.2007.10.063
7. Bhide SA, Davies M, Burke K, McNair HA, Hansen V, Barbachano Y, et al. Weekly volume and dosimetric changes during chemoradiotherapy with intensity-modulated radiation therapy for head and neck cancer: a prospective observational study. *Int J Radiat Oncol Biol Phys* 2010; **76**: 1360–8. doi: http://dx.doi.org/10.1016/j.ijrobp.2009.04.005
8. Marzi S, Pinnaro P, D'Alessio D, Strigari L, Bruzzaniti V, Giordano C, et al. Anatomical and dose changes of gross tumour volume and parotid glands for head and neck cancer patients during intensity-modulated radiotherapy: effect on the probability of xerostomia incidence. *Clin Oncol (R Coll Radiol)* 2012; **24**: e54–62. doi: http://dx.doi.org/10.1016/j.clon.2011.11.006
9. Loo H, Fairfoul J, Chakrabarti A, Dean JC, Benson RJ, Jefferies SJ, et al. Tumour shrinkage and contour change during radiotherapy increase the dose to organs at risk but not the target volumes for head and neck cancer patients treated on the TomoTherapy HiArt™ system. *Clin Oncol (R Coll Radiol)* 2011; **23**: 40–7. doi: http://dx.doi.org/10.1016/j.clon.2010.09.003
10. Castadot P, Geets X, Lee JA, Christian N, Grégoire V. Assessment by a deformable registration method of the volumetric and positional changes of target volumes and organs at risk in pharyngo-laryngeal tumors treated with concomitant chemo-radiation. *Radiother Oncol* 2010; **95**: 209–17. doi: http://dx.doi.org/10.1016/j.radonc.2010.03.007
11. Hansen EK, Bucci MK, Quivey JM, Weinberg V, Xia P. Repeat CT imaging and replanning during the course of IMRT for head-and-neck cancer. *Int J Radiat Oncol Biol Phys* 2006; **64**: 355–62. doi: http://dx.doi.org/10.1016/j.ijrobp.2005.07.957
12. O'Daniel JC, Garden AS, Schwartz DL, Wang H, Ang KK, Ahamad A, et al. Parotid gland dose in intensity-modulated radiotherapy for head and neck cancer: is what you plan what you get? *Int J Radiat Oncol Biol Phys* 2007; **69**: 1290–6. doi: http://dx.doi.org/10.1016/j.ijrobp.2007.07.2345
13. Wang W, Yang H, Hu W, Shan G, Ding W, Yu C, et al. Clinical study of the necessity of replanning before the 25th fraction during the course of intensity-modulated radiotherapy for patients with nasopharyngeal carcinoma. *Int J Radiat Oncol Biol Phys* 2010; **77**: 617–21. doi: http://dx.doi.org/10.1016/j.ijrobp.2009.08.036
14. Lee C, Langen KM, Lu W, Haimerl J, Schnarr E, Ruchala KJ, et al. Assessment of parotid gland dose changes during head and neck cancer radiotherapy using daily megavoltage computed tomography and deformable image registration. *Int J Radiat Oncol Biol Phys* 2008; **71**: 1563–71. doi: http://dx.doi.org/10.1016/j.ijrobp.2008.04.013
15. Wu Q, Chi Y, Chen PY, Krauss DJ, Yan D, Martinez A. Adaptive replanning strategies accounting for shrinkage in head and neck IMRT. *Int J Radiat Oncol Biol Phys* 2009; **75**: 924–32. doi: http://dx.doi.org/10.1016/j.ijrobp.2009.04.047
16. Chen AM, Daly ME, Cui J, Mathai M, Benedict S, Purdy JA. Clinical outcomes among patients with head and neck cancer treated by intensity-modulated radiotherapy with and without adaptive replanning. *Head Neck* 2014; **36**: 1541–6. doi: http://dx.doi.org/10.1002/hed.23477
17. Schwartz DL, Garden AS, Shah SJ, Chronowski G, Sejpal S, Rosenthal DI, et al. Adaptive radiotherapy for head and neck cancer—dosimetric results from a prospective clinical trial. *Radiother Oncol* 2013; **106**: 80–4. doi: http://dx.doi.org/10.1016/j.radonc.2012.10.010
18. Castelli J, Simon A, Louvel G, Henry O, Chajon E, Nassef M, et al. Impact of head and neck cancer adaptive radiotherapy to spare the parotid glands and decrease the risk of xerostomia. *Radiat Oncol* 2015; **10**: 6. doi: http://dx.doi.org/10.1186/s13014-014-0318-z
19. Ahn PH, Chen CC, Ahn AI, Hong L, Scripes PG, Shen J, et al. Adaptive planning in intensity-modulated radiation therapy for head and neck cancers: single-institution experience and clinical implications. *Int J Radiat Oncol Biol Phys* 2011; **80**: 677–85. doi: http://dx.doi.org/10.1016/j.ijrobp.2010.03.014
20. Schwartz DL, Garden AS, Thomas J, Chen Y, Zhang Y, Lewin J, et al. Adaptive radiotherapy for head-and-neck cancer: initial clinical outcomes from a prospective trial. *Int J Radiat Oncol Biol Phys* 2012; **83**: 986–93. doi: http://dx.doi.org/10.1016/j.ijrobp.2011.08.017
21. Dirix P, Haustermans K, Vandecaveye V. The value of magnetic resonance imaging for radiotherapy planning. *Semin Radiat Oncol* 2014; **24**: 151–9. doi: http://dx.doi.org/10.1016/j.semradonc.2014.02.003
22. Chen AM, Li J, Beckett LA, Zhara T, Farwell G, Lau DH, et al. Differential response rates to irradiation among patients with human papillomavirus positive and negative oropharyngeal cancer. *Laryngoscope* 2013; **123**:

152–7. doi: http://dx.doi.org/10.1002/lary.23570
23. Noel CE, Parikh PJ, Spencer CR, Green OL, Hu Y, Mutic S, et al. Comparison of onboard low-field magnetic resonance imaging *versus* onboard computed tomography for anatomy visualization in radiotherapy. *Acta Oncol* 2015; **54**: 1474–82. doi: http://dx.doi.org/10.3109/0284186X.2015.1062541
24. Devic S. MRI simulation for radiotherapy treatment planning. *Med Phys* 2012; **39**: 6701–11. doi: http://dx.doi.org/10.1118/1.4758068
25. Mutic S, Dempsey JF. The ViewRay system: magnetic resonance-guided and controlled radiotherapy. *Semin Radiat Oncol* 2014; **24**: 196–9. doi: http://dx.doi.org/10.1016/j.semradonc.2014.02.008
26. Kamran SC, Tyagi N, Han J, McBride S, Riaz N, Lee N. Weekly on-treatment MRIs during radiation therapy (RT) in head and neck squamous cell carcinoma (HNSCC) patients to monitor treatment response. *Int J Radiat Oncol Biol Phys* 2014; **90**: S516. doi: http://dx.doi.org/10.1016/j.ijrobp.2014.05.1580
27. Ho KF, Marchant T, Moore C, Webster G, Rowbottom C, Penington H, et al. Monitoring dosimetric impact of weight loss with kilovoltage (kV) cone beam CT (CBCT) during parotid-sparing IMRT and concurrent chemotherapy. *Int J Radiat Oncol Biol Phys* 2012; **82**: e375–82. doi: http://dx.doi.org/10.1016/j.ijrobp.2011.07.004
28. Robar JL, Day A, Clancey J, Kelly R, Yewondwossen M, Hollenhorst H, et al. Spatial and dosimetric variability of organs at risk in head-and-neck intensity-modulated radiotherapy. *Int J Radiat Oncol Biol Phys* 2007; **68**: 1121–30. doi: http://dx.doi.org/10.1016/j.ijrobp.2007.01.030
29. Weygand J, Fuller CD, Ibbott GS, Mohamed AS, Ding Y, Yang J, et al. Spatial precision in magnetic resonance imaging-guided radiation therapy: the role of geometric distortion. *Int J Radiat Oncol Biol Phys* 2016; **95**: 1304–16. doi: http://dx.doi.org/10.1016/j.ijrobp.2016.02.059
30. Stanescu T, Wachowicz K, Jaffray DA. Characterization of tissue magnetic susceptibility-induced distortions for MRIgRT. *Med Phys* 2012; **39**: 7185–93. doi: http://dx.doi.org/10.1118/1.4764481
31. Petersch B, Bogner J, Fransson A, Lorang T, Pötter R. Effects of geometric distortion in 0.2T MRI on radiotherapy treatment planning of prostate cancer. *Radiother Oncol* 2004; **71**: 55–64. doi: http://dx.doi.org/10.1016/j.radonc.2003.12.012
32. Crijns SP, Bakker CJ, Seevinck PR, de Leeuw H, Lagendijk JJ, Raaymakers BW. Towards inherently distortion-free MR images for image-guided radiotherapy on an MRI accelerator. *Phys Med Biol* 2012; **57**: 1349–58. doi: http://dx.doi.org/10.1088/0031-9155/57/5/1349
33. Zhang Y, Guo CB, Zhang L, Wang Y, Peng X, Mao C, et al. Prevention of radiation-induced xerostomia by submandibular gland transfer. *Head Neck* 2012; **34**: 937–42. doi: http://dx.doi.org/10.1002/hed.21859